Flo11p, drug efflux pumps, and the extracellular matrix cooperate to form biofilm yeast colonies

Libuše Váchová,[1,2] Vratislav Šťovíček,[2] Otakar Hlaváček,[1] Oleksandr Chernyavskiy,[3] Luděk Štěpánek,[2] Lucie Kubínová,[3] and Zdena Palková[2]

[1]Institute of Microbiology of the Academy of Sciences of the Czech Republic, v.v.i., 142 20 Prague, Czech Republic
[2]Faculty of Science, Charles University in Prague, 128 44 Prague, Czech Republic
[3]Institute of Physiology of the Academy of Sciences of the Czech Republic, v.v.i., 142 20 Prague, Czech Republic

Much like other microorganisms, wild yeasts preferentially form surface-associated communities, such as biofilms and colonies, that are well protected against hostile environments and, when growing as pathogens, against the host immune system. However, the molecular mechanisms underlying the spatiotemporal development and environmental resistance of biofilms and colonies remain largely unknown. In this paper, we show that a biofilm yeast colony is a finely tuned, complex multicellular organism in which specialized cells jointly execute multiple protection strategies. These include a Pdr1p-regulated mechanism whereby multidrug resistance transporters Pdr5p and Snq2p expel external compounds solely within the surface cell layers as well as developmentally regulated production by internal cells of a selectively permeable extracellular matrix. The two mechanisms act in concert during colony development, allowing growth of new cell generations in a well-protected internal cavity of the colony. Colony architecture is strengthened by intercellular fiber connections.

Introduction

In natural environments, microorganisms preferentially form organized multicellular communities, such as biofilms and colonies. These structures possess unique attributes that provide resistance against chemicals and other threats and also adaptability to changing conditions, allowing the community to survive in a hostile natural environment (Donlan and Costerton, 2002; Palková, 2004). Features implicated as being essential for the formation of complex fungal biofilms include adhesion to surfaces, the production of an ECM, multidrug resistance (MDR) plasma membrane transporters, and specialized cell subpopulations, such as stationary cells that are more resistant to various stresses (Douglas, 2003; Blankenship and Mitchell, 2006).

Cell–cell and cell–surface adhesion are often mediated by specific cell wall–adhesive glycophosphatidylinositol-anchored proteins (Dranginis et al., 2007). In *Saccharomyces cerevisiae*, the FLO family of protein adhesins is considered the most important, with pleiotropic Flo11p involved in cell adhesion to inert substrates (Verstrepen et al., 2004), filamentous growth (Lambrechts et al., 1996), and the formation of structured colonies (Vopálenská et al., 2010), flor biofilms (Ishigami et al., 2004), and mats (Reynolds and Fink, 2001). In contrast to Flo1p, Flo5p, and Flo9p, which are crucial for cell–cell adhesion during flocculation (Guo et al., 2000), the role of Flo11p in this process is strain specific (Bayly et al., 2005; Douglas et al., 2007). The ALS family and Hwp1p, which are related to FLO adhesins, mediate the adhesion of *Candida albicans* and are important for normal biofilm development (Nobile et al., 2008).

An ECM is exclusively present in structured *S. cerevisiae* colonies but not in their domesticated counterparts (Kuthan et al., 2003), and it is found in air–liquid flor biofilms (Zara et al., 2009). In addition, flocculating *S. cerevisiae* cells expressing the *FLO1* gene secrete a mixture of polysaccharides that blocks the permeation of large molecules (e.g., antibodies; Beauvais et al., 2009). In addition to these findings in *S. cerevisiae* populations, an ECM is regularly encountered in biofilms of *Candida* species (Baillie and Douglas, 2000). In both structured *S. cerevisiae* colonies and yeast biofilms, the ECM facilitates

L. Váchová and Z. Palková contributed equally to this paper.

Correspondence to Zdena Palková: zdenap@natur.cuni.cz; or Libuše Váchová: vachova@biomed.cas.cz

Abbreviations used in this paper: 2P-CM, two-photon excitation confocal microscopy; MDR, multidrug resistance; NR, Nile red.

© 2011 Váchová et al. This article is distributed under the terms of an Attribution–Noncommercial–Share Alike–No Mirror Sites license for the first six months after the publication date (see http://www.rupress.org/terms). After six months it is available under a Creative Commons License (Attribution–Noncommercial–Share Alike 3.0 Unported license, as described at http://creativecommons.org/licenses/by-nc-sa/3.0/).

The Rockefeller University Press $30.00
J. Cell Biol. Vol. 194 No. 5 679–687
www.jcb.org/cgi/doi/10.1083/jcb.201103129

THE JOURNAL OF CELL BIOLOGY

Downloaded from http://rupress.org/jcb/article-pdf/194/5/679/1569090/jcb_201103129.pdf by guest on 06 December 2025

the formation of pores for water and nutrient flow (Douglas, 2003; Kuthan et al., 2003) and protects the communities against dehydration (Flemming and Wingender, 2010).

S. cerevisiae MDR transporters belonging to the ATP-binding cassette family are involved in the ATP-dependent efflux of a wide variety of unrelated compounds, including drugs and other noxious substances. Deletions of these pumps lead to the cells becoming drug hypersensitive (Rogers et al., 2001; Sipos and Kuchler, 2006). The function of the MDR pumps in *S. cerevisiae* multicellular structures has not yet been examined. Flocculating cells up-regulate some MDR transporter genes (Smukalla et al., 2008), but their function in floc resistance remains undocumented. It has been shown, however, that *C. albicans* biofilms increase their expression of the MDR genes *CDR1*, *CDR2*, and *MDR1* (Ramage et al., 2002), and deletions of these genes decrease the resistance of biofilms (Mukherjee et al., 2003).

In contrast to the smooth colonies of laboratory strains, wild *S. cerevisiae* strains form structured colonies possessing attributes common to fungal biofilms and are hence referred to as biofilm colonies. Their attributes include the production of an ECM rich in polysaccharides and high water retention capacity and the production of the adhesin Flo11p for substrate adhesion and 3D architecture formation (Šťovíček et al., 2010). Using two-photon excitation confocal microscopy (2P-CM; Váchová et al., 2009) in combination with fluorescent protein tagging and staining methods, we show here the dynamics of colony development. Colony structure was composed of an aerial part with an internal cavity and subsurface pseudohyphae, was strengthened by intercellular fibers formed in the presence of Flo11p, and was protected by Pdr5p and Snq2p transporters together with an ECM that was secreted by internal cells.

Results and discussion

Spatiotemporal architecture of a biofilm colony

Examining the population of a wild *S. cerevisiae* BR-F strain, we show (Fig. 1) that a 25-h-old population of mostly rounded cells had already formed a small colony with short pseudohyphae (i.e., elongated cells joined into filaments; Gimeno et al., 1992) invading the agar at its base. Several hours later, an internal cavity appeared within the mound colony (Fig. 1 A, 34–42 h). The colony then expanded primarily horizontally with an elevated ridge at its margin (Fig. 1 A, the earlike structure in the cross section) and an internal cavity (Fig. 1 A, 48–60 h). The colony also formed abundant rootlike pseudohyphae that grew radially into the agar from its central bottom region (Fig. 1, A and B). Later, the central colony area further expanded horizontally, pushing the ridge apart (Fig. 1 A, 3 d), and the colony became cup shaped (Fig. S1 A). During this period, secondary roots began to grow from the base of the ridge, anchoring it to the agar. The continued horizontal growth of the central cell layer thereby led to its undulation and the formation of wrinkles (Fig. 1 A, 7 d; and Video 1), as also observed in some types of biofilms (Uppuluri et al., 2009). The architecture of structured colonies formed by various wild *S. cerevisiae* strains is comparable, thus indicating universal underlying principles.

The cells within colonies are interconnected by long, thin fibers that extend from cell walls and form a velcrolike structure (Figs. 1 E and S1 B). The fibers interconnect oval cells in the upper layer and pseudohyphae in the roots (Fig. S1 B). They can hold cells close to one another but can also be stretched up to 460 nm. These fibrous interconnections appear to be composed of two halves, each belonging to one of the interconnected cells, as they are more electron dense in the adhesion area. Adhesin Flo11p participates in the formation of the fibers, which are absent in colonies from the strain lacking Flo11p (BR-F–*flo11*; Fig. S1 B). Two Flo11p molecules are long enough to form a fiber interconnection 460 nm long, even if they are partially coiled, and they may aggregate into bundles via amyloid formation (Ramsook et al., 2010). Alternatively, the effect of Flo11p could be indirect, e.g., eliciting a change that leads to the production of other surface adhesins. The finding of velcrolike interconnections is of particular interest in *C. albicans*, in which brushlike fibrillar structures composed of long fibers (100–160 nm) were observed on the surface of cells growing in liquid cultures (Tokunaga et al., 1986), and an involvement of adhesins has been proposed (Klis et al., 2009). Much shorter fibers related to Flo1p were observed on the surface of flocculating *S. cerevisiae* cells (Beauvais et al., 2009).

To distinguish between the areas of dividing and stationary cells within the developing colony, we used two detection systems: (1) a BR-F–Hmg1p-GFP strain with a GFP gene fused to the *HMG1* gene encoding the hydroxymethylglutaryl-CoA reductase of the nuclear envelope (Koning et al., 1996), which exhibits typical distributions in dividing and stationary cells (Fig. 2 B), and (2) the BR-F–cdc3^{ts} strain with the ts mutation in the *CDC3* gene for septin (Fig. 2 A; Hartwell, 1971). Dividing cells were spread uniformly throughout the colonies that were 24–36 h old (Fig. 2 C). Beginning at ∼40 h, the colony became stratified with the upper cells becoming mostly stationary while the rest of the colony contained dividing cells (Fig. 2 D). In colonies that were 3 d old, the surface layers of the ridge and central plateau mostly consisted of stationary cells. The internal layers consisted of sporadically or slowly dividing, but still relatively young, cells, whereas only the ridge interior and the root bases and tips still contained actively dividing cells (Fig. 1, C and D). These observations demonstrate that clearly demarcated zones of dividing and nondividing cells are discernible within the structured colonies (Fig. 1 F).

Structured colony defense by MDR pumps

Unlike the smooth laboratory strain colony (Váchová et al., 2009), the biofilm colony was not covered by a protective cell monolayer (unpublished data). However, we did identify a distinct property of the surface cell layers that was important for protecting the population as a whole. Surface cells (visualized by ConA-AF [ConA conjugated with Alexa Fluor 488] cell wall staining in vertical transverse colony cross sections) could not be stained with Nile red (NR), which targets lipid granules and membranes (Greenspan and Fowler, 1985). This NR-free cell layer was present throughout the BR-F colony (Fig. 3, A and B),

Downloaded from http://rupress.org/jcb/article-pdf/194/5/679/1569090/jcb_201103129.pdf by guest on 06 December 2025

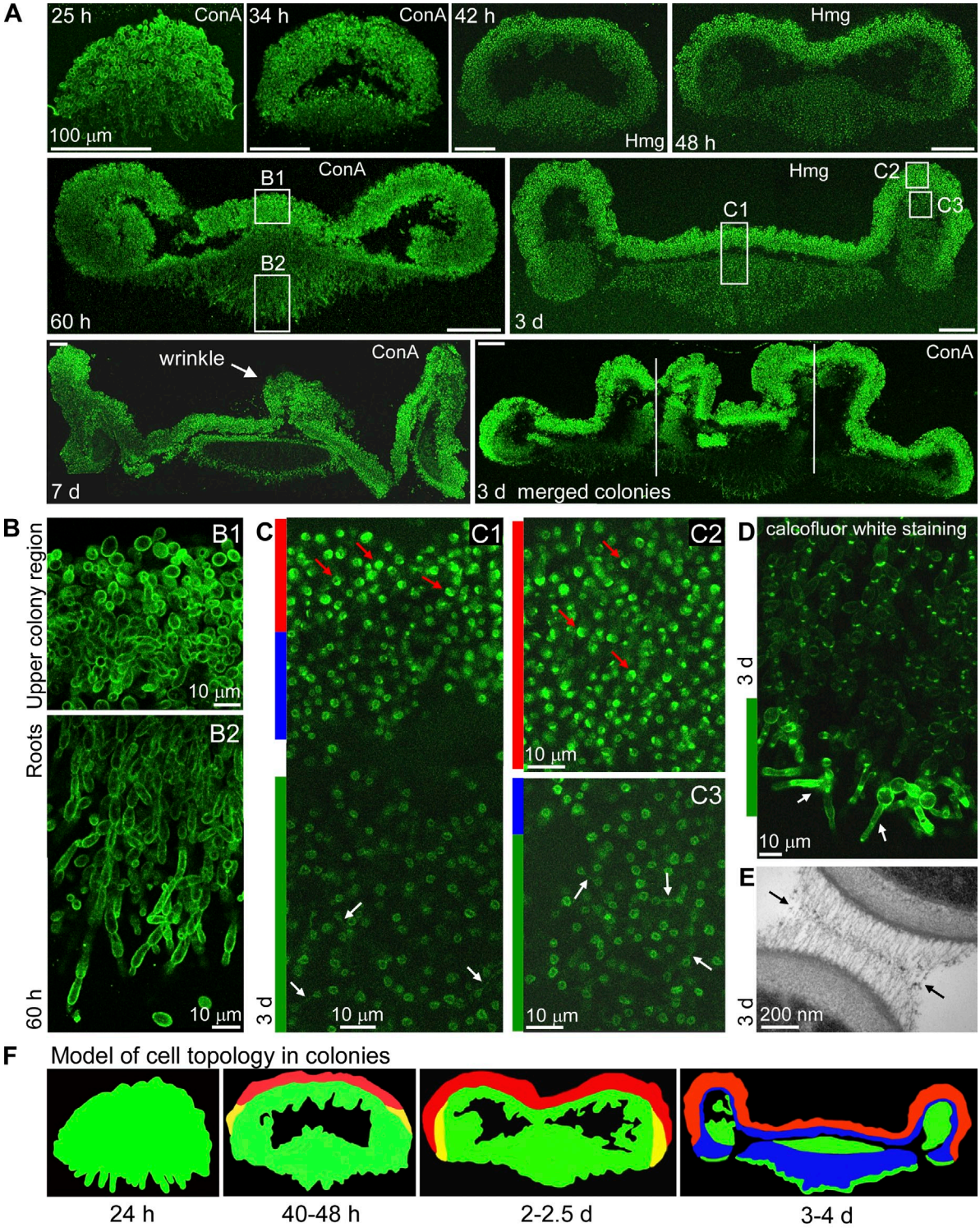

Figure 1. **Colony architecture and topology of different cell types.** (A) Vertical transverse cross sections of BR-F colonies stained with ConA-AF (ConA) and BR-F–Hmg1p-GFP (Hmg) colonies. Vertical white lines mark the borders of three individual colonies. (B) Typical morphology of cells in roots and the upper colony region (magnified regions are marked in A). (C) Cell morphology in BR-F–Hmg1p-GFP colonies. Areas with stationary (red bar), dividing (green bar), and young nondividing (blue bar) cells are shown. Arrows indicate examples of dividing (white) and stationary (red) cells (magnified regions are marked in A). (D) Distribution of dividing cells in root tips of BR-F–cdc3^{ts} colonies. Examples of cells reaching a terminal phenotype (Fig. 2 A) are marked by arrows. (E) Velcrolike interconnection (marked by arrows) between cells in the upper central region of 3-d-old colonies visualized by EM (more in Fig. S1). (F) Diagrammatic illustrations of the cell topology in the course of colony development (based on BR-F–Hmg1p-GFP and BR-F–cdc3^{ts} data; also see Fig. 2). Regions with dividing (green), early stationary (yellow), stationary (red), and younger with no apparent division activity (blue) cells are shown. Two (A, 60 h and 3 d) or three (A, 7- and 3-d merged colonies) individual images spanning the width of the colony were acquired and assembled after acquisition to generate the composite image shown. Details in B2 and C1 were obtained by composing two images of neighboring fields of view.

Downloaded from http://rupress.org/jcb/article-pdf/194/5/679/1569090/jcb_201103129.pdf by guest on 06 December 2025

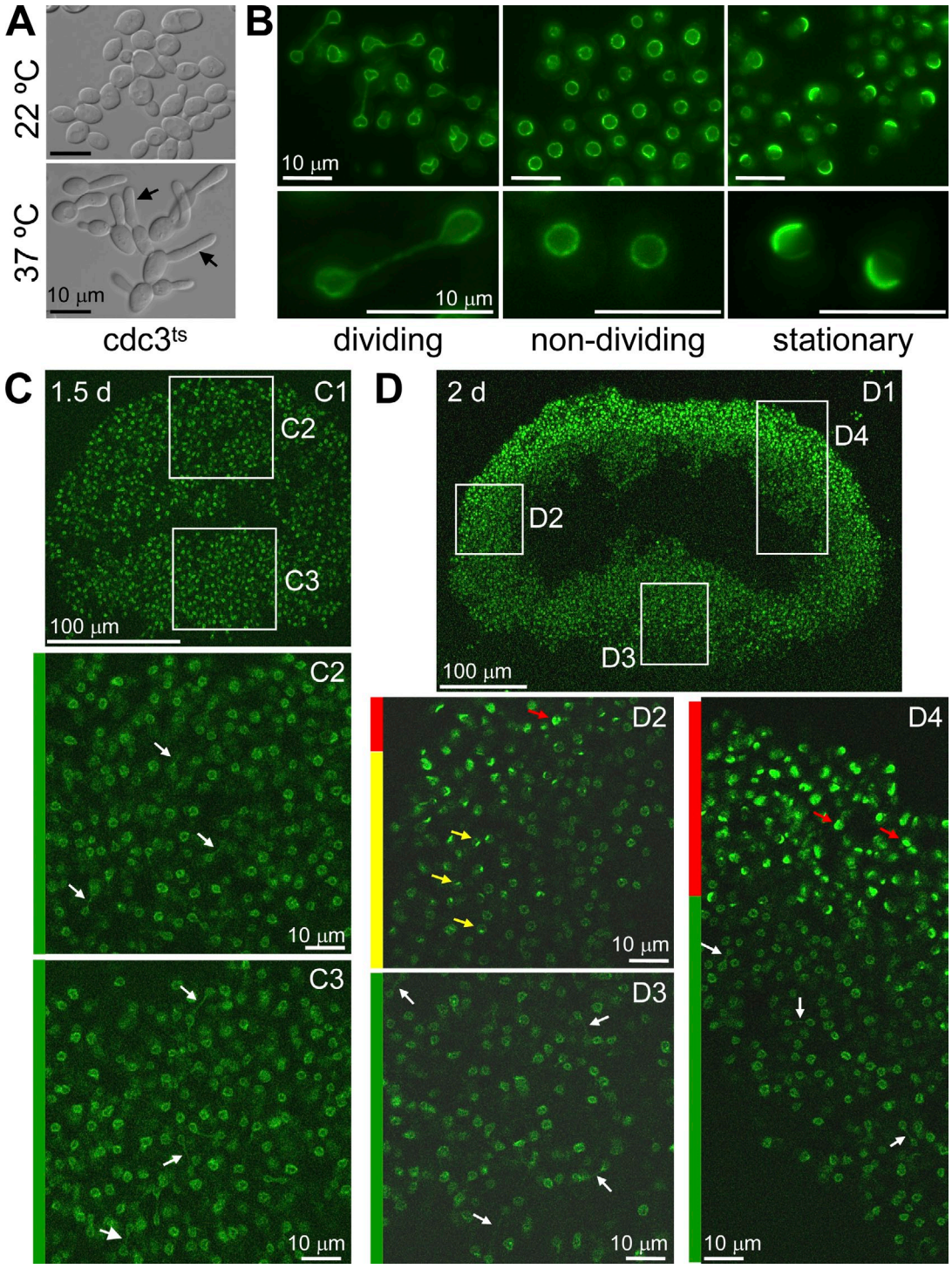

Figure 2. **Topology of dividing and stationary cells in colonies.** (A and B) Visualization of dividing, nondividing, and stationary cells. (A) Morphology of BR-F–cdc3^{ts} cells from liquid cultures grown for 2 h at permissive (22°C) and nonpermissive (37°C) temperature. Arrows indicate a typical morphology reached by dividing cells at 37°C. (B) Distribution of Hmg1p-GFP in dividing, nondividing, and stationary cells grown in liquid medium. (C and D) Cell topology in BR-F–Hmg1p-GFP colonies. Areas with stationary (red bars and arrows), early stationary (yellow bar and arrows), and dividing (green bars and white arrows) cells are shown. Arrows mark typical cell types. Magnified regions are marked with boxes. (C) A 1.5-d-old colony. (D) A 2-d-old colony. The detail in D4 was obtained by composing two images of neighboring fields of view.

including the pseudohyphae tips (Fig. 3 C). This layer was thick (17.8 ± 2.5 μm) in colonies 24–36 h old, persisted over the next 2 d, became thinner in the aerial part (11.5 ± 1.2 μm in a colony 3 d old), and, with the exception of the root tips, disappeared in older colonies (7 d old). After formaldehyde fixation or treatment with NaN_3 causing rapid cellular ATP depletion, entire colonies could be stained with NR (Fig. 3 D). This demonstrated that lipid particles are present in untreated colonies, but NR is probably removed from the surface cells. We considered MDR pumps to be prime candidates for this

Downloaded from http://rupress.org/jcb/article-pdf/194/5/679/1569090/jcb_201103129.pdf by guest on 06 December 2025

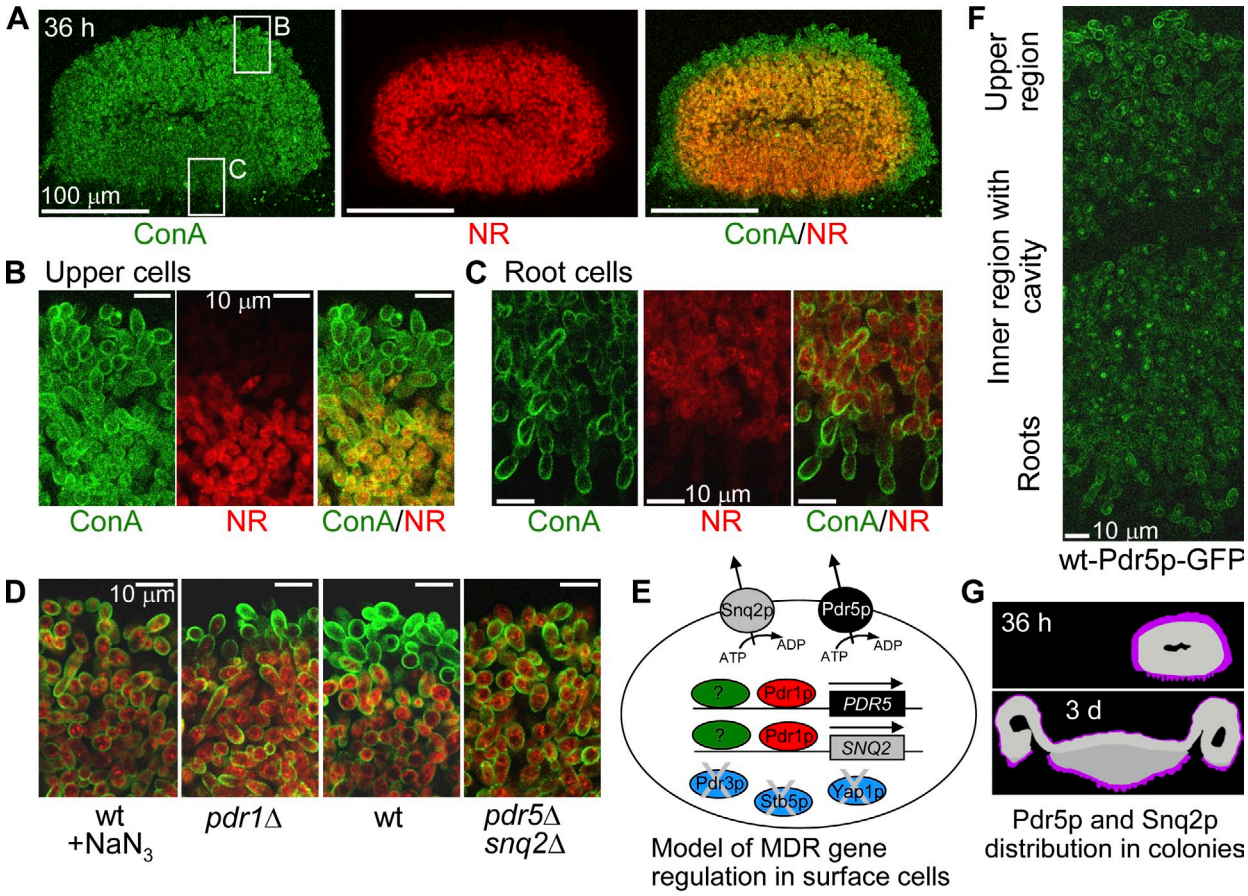

H

STRAIN	wt	*pdr1*	*pdr3*	*pdr1 pdr3*	*pdr5*	*pdr5 snq2*	*pdr1 yap1*	*pdr1 stb5*	Pdr5p -GFP	Snq2p -GFP	Pdr10p -GFP	Pdr15p -GFP
NR extrusion	+	±	+	±	±	-	±	±				
Transporter localization[1]									YES	ND[2]	ND[2]	ND[2]

[1] Transporter in the plasma membrane of cells localized in the surface layer of colonies 1.5 d old
[2] GFP fluorescence signal not detected.

Figure 3. **Localization of active MDR pumps within colonies.** (A–D) Vertical transverse cross sections of BR-F colonies that were 36 h old, stained with ConA-AF (ConA) and NR. (A) A layer of NR-free cells covers the entire colony. (B and C) Details of the upper (B) and root (C) cells from the boxes in A are shown. (D) NR extrusion by the surface cell layer is reduced by removing the transcription factor Pdr1p and blocked by energy depletion (using NaN_3) or the absence of both Pdr5p and Snq2p MDR transporters. (E) A model of MDR gene regulation. (F) Pdr5p-GFP localization in the membrane of the upper cells and root tips compares well with that in the NR-free colony layer in A–C. (G) A model of Pdr5p and Snq2p distribution (violet) in colonies. (H) NR extrusion and transporter localization in colonies of different strains. wt, wild type.

process. Indeed, the disruption of the *PDR1* gene, encoding a transcription activator of some MDR transporters (Balzi et al., 1987; Fardeau et al., 2007), significantly diminished the removal of NR (Fig. 3 D). Deleting various combinations of genes coding for individual MDR pumps (Snq2p [Servos et al., 1993], Pdr5p [Balzi et al., 1994], and the latter's close relatives Pdr10p and Pdr15p [Wolfger et al., 1997]; Fig. 3 H and Table I) demonstrated that Pdr5p and Snq2p are essential for the extrusion of NR from the surface cells of colonies, as dye export was completely blocked in the BR-F–*pdr5snq2* strain (Fig. 3 D). Moreover, we demonstrated that the Pdr5p-GFP transporter was mainly present in the plasma membrane of cells located at the surface of BR-F–Pdr5p-GFP colonies that were 1.5 d old. Meanwhile, internal cells exhibited mostly vacuolar GFP fluorescence, which is indicative of Pdr5p degradation (Fig. 3 F). Deletions of other potential MDR regulator genes, *PDR3*, *STB5*, and *YAP1* (Jungwirth and Kuchler, 2006), in the BR-F–*pdr1* strain had no effect on Pdr5p/Snq2p function (Fig. 3 H). This indicates that the expression of *PDR5* and *SNQ2* in the surface layer of BR-F colonies is regulated by the Pdr1p transcription factor, probably jointly with an additional, yet unidentified, MDR gene regulator (Fig. 3 E). Together, these findings imply an important protective role of the surface cells equipped with Pdr5p, Snq2p, and possibly other MDR exporters in the removal of external toxic compounds (Fig. 3 G).

Downloaded from http://rupress.org/jcb/article-pdf/194/5/679/1569090/jcb_201103129.pdf by guest on 06 December 2025

Table I. **Yeast strains used in this study**

Name	Genotype	Source
BR-F	*MATa/MATα*	Institute of Chemistry, Slovak Academy of Sciences (collection no. CCY 21-4-97)
ts104	*MATa adelΔ ade2Δ uralΔ tyrlΔ his7Δ lysΔ gallΔ cdc3-1*	Charles University in Prague (collection no. DMUP 12-4-80)
BR-F–*pdr1*[a]	*MATa/MATα pdr1Δ::kanMX/pdr1Δ::nat1*	This study
BR-F–*pdr3*[a]	*MATa/MATα* pdr3Δ::*kanMX*/pdr3Δ::*nat1*	This study
BR-F–*pdr1pdr3*[a]	*MATa/MATα pdr1Δ::kanMX*/pdr1Δ::*nat1 pdr3Δ::hph*/pdr3Δ::*ble*	This study
BR-F–*pdr5*[a]	*MATa/MATα pdr5Δ::kanMX/pdr5Δ::nat1*	This study
BR-F–*pdr5snq2*[a]	*MATa/MATα pdr5Δ::kanMX/pdr5Δ::nat1 snq2Δ::hph/snq2Δ::ble*	This study
BR-F–*pdr1yap1*[a]	*MATa/MATα pdr1Δ::kanMX/pdr1Δ::nat1 yap1Δ::hph/yap1Δ::ble*	This study
BR-F–*pdr1stb5*[a]	*MATa/MATα pdr1Δ::kanMX/pdr1Δ::nat1 stb5Δ::hph/stb5Δ::ble*	This study
BR-F–P_{CUP1}-GFP[a]	*MATa/MATα HIS3/his3Δ::nat1*-P_{CUP1}-GFP	This study
BR-F–P_{GAL1}-GFP[a]	*MATa/MATα HIS3/his3Δ::nat1*-P_{GAL1}-GFP	This study
BR-F–Hmg1p-GFP[a]	*MATa/MATα HMG1*-EGFP-*kanMX/HMG1*	This study
BR-F–Pdr5p-GFP[a]	*MATa/MATα PDR5*-EGFP-*kanMX/PDR5*	This study
BR-F–Snq2p-GFP[a]	*MATa/MATα SNQ2*-EGFP-*kanMX/SNQ2*	This study
BR-F–Pdr10p-GFP[a]	*MATa/MATα PDR10*-EGFP-*kanMX/PDR10*	This study
BR-F–Pdr15p-GFP[a]	*MATa/MATα PDR15*-EGFP-*kanMX/PDR15*	This study
BR-F–*cdc3CDC3*[a]	*MATa/MATα cdc3Δ::kanMX/CDC3*	This study
BR-F–cdc3[ts b]	*MATa/MATα cdc3Δ::kanMX/cdc3-1-nat1*	This study
BR-F–*flo11*[c]	*MATa/MATα flo11Δ::kanMX/flo11Δ::ble*	This study

[a]Forms structured colonies. Their morphology is identical to that of the parental BR-F strain.
[b]Colonies grow more slowly at 22°C. Their morphology is identical to that of the parental BR-F strain.
[c]Forms smooth colonies.

Nutrient flow in the colony and its protection by ECM

In contrast to the tightly packed cells within smooth colonies, pores are present within structured colonies (Kuthan et al., 2003) that are similar to those allowing nutrient flow in biofilms (Douglas, 2003). To study nutrient flow within the biofilm colony, we set up detection systems based on the expression of GFP under the control of a regulatable promoter, P_{GAL1} or P_{CUP1}, in the BR-F strain (Table I). 45 min after feeding the colonies of such strains with the inductor (galactose or copper ions) from the agar side, GFP fluorescence was detected not only in the tips of the pseudohyphae (i.e., closest to the inductor) but also in all of the cells in the surface layer, implying a very efficient propagation of the inductor within the colony. Surprisingly, a majority of the root cells and internal parts of the ridge remained uninduced even after 5 h of induction (Fig. 4 A). However, all colony cells were induced when the exposed vertical transverse cross section of the colony was placed flat on agar soaked with the inductor (Fig. 4 C). Therefore, we hypothesize that the uninduced part of the colony produces an ECM (different from the velcrolike fibers that are present throughout the entire colony), completely blocking the penetration of certain chemical species, even small ones, to the inner parts of the intact colony. The low-permeable ECM begins to be produced in the central area of young (33–35 h old) colonies, and the area expands with the colony growth (Fig. 4 B).

In contrast to the zones of stationary cells that appear in the air-facing aerial part of the colony, the ECM prevents the penetration of chemicals from both the aerial and subsurface colony parts. The existence of the ECM is supported by the earlier scanning EM observation of an abundant extracellular material containing a sugar component (Kuthan et al., 2003). A microscopically similar ECM of *C. albicans* species biofilm (Al-Fattani and Douglas, 2006) and the extracellular glucan of *C. albicans* biofilm sequestering antifungals (Nett et al., 2010) both contribute to the biofilm drug resistance.

A model of biofilm colony formation and protection

These developmental principles, as revealed in this study, provide new insights into the differentiation of a biofilm colony and the function of specialized cell subpopulations, and they suggest the presence of unique mechanisms of population protection (Video 2). What are the colony strategies? A colony arising from a single cell grows very quickly, as most cells efficiently divide. In contrast to a smooth laboratory strain colony, biofilm colony also expands substantially in the vertical direction. This expansion may be enabled by the velcrolike interconnection of its cells. Initially, the colony population protects itself from external chemical threats by inducing MDR exporters (Fig. S2) capable of removing toxic compounds (Sipos and Kuchler, 2006). Later, the activity of the exporters persists exclusively in the surface cell layers over the entire colony, and, in parallel, additional protection strategies are initiated. The upper cell layers of the aerial part of the colony become stationary and thus more resistant to chemical and other threats. As the nutrients from agar are efficiently transported, the formation of such nondividing cells appears to be not simply the result of nutrient exhaustion but, more likely, a regulated process that helps to protect the colony surface that is directly exposed to the open air. In parallel, the internal cells near the agar begin to produce the ECM.

The preservation of the velcrolike joints then contributes to the mechanical stability of the expanding colony and may

Downloaded from http://rupress.org/jcb/article-pdf/194/5/679/1569090/jcb_201103129.pdf by guest on 06 December 2025

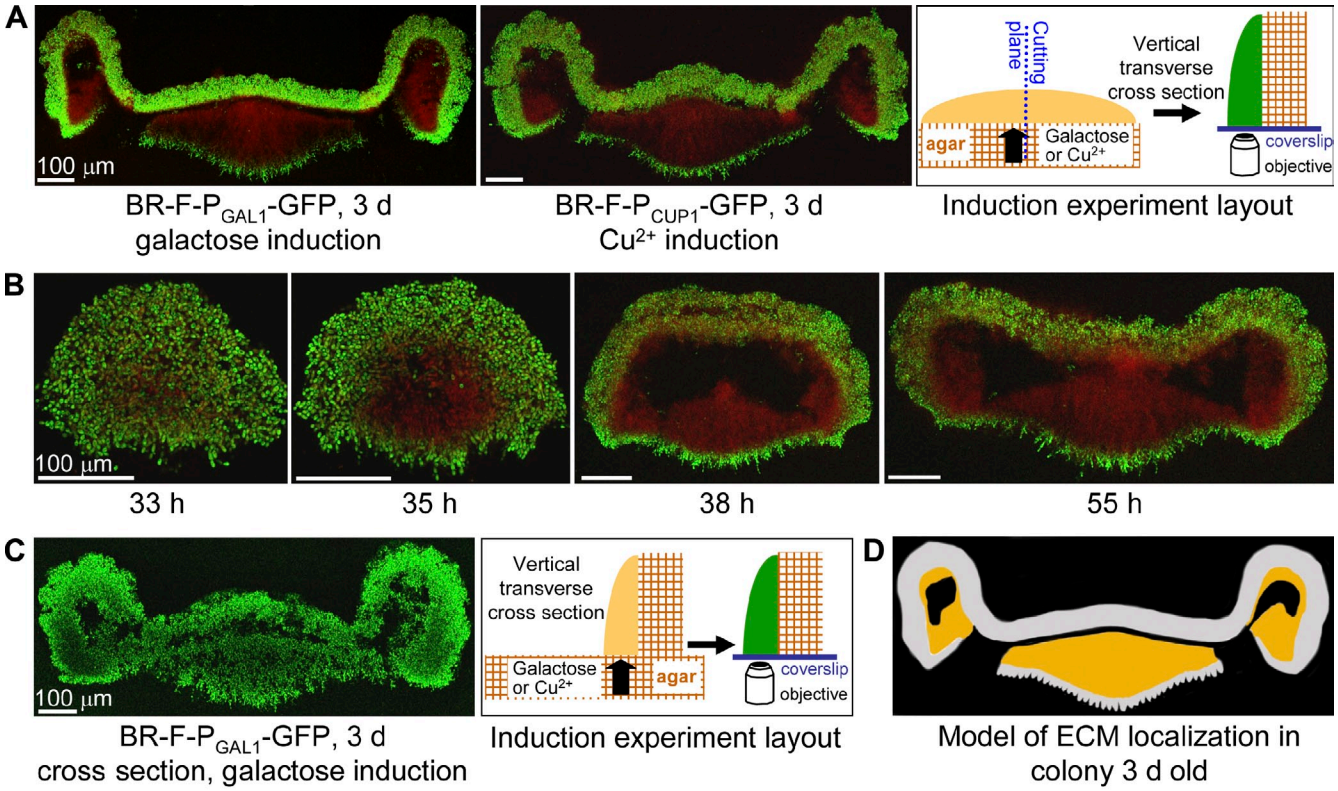

Figure 4. **Nutrient flow and localization of ECM within colonies.** Vertical transverse colony cross sections. (A) Areas of galactose or Cu^{2+} induction in colonies (the vertical arrow indicates diffusion into the colony). (B) Timeline of ECM formation. (A and B) Green, GFP fluorescence marks areas in which the inducer reached the cells; red, autofluorescence of all colony cells visible in areas where ECM prevented the inducer from accessing the cells. Intact colonies were induced from the bottom by placing them for 5 h on agar soaked with 2% galactose or 5 mM $CuSO_4$. GFP fluorescence was detectable by 2P-CM as early as 45 min after induction. (C) The exposed area of the vertical transverse colony section was placed flat on galactose-soaked agar (a 2-h induction), after which internal cells were induced as well. (D) A model scheme featuring impermeable ECM (yellow). Two (B [55 h] and C) or three (A) individual images spanning the width of the colony were acquired and assembled after acquisition to generate the composite image shown.

lend flexibility to the layer, forming aerial wrinkles with internal cavities. Subsequent cell generations formed by the dividing inner cells of that layer are thus well protected. The cells in the inner bottom part of the ridge and the pseudohyphae in the subsurface colony regions do not enter a stationary phase. Rather, they continue to produce the ECM that is impermeable to some small compounds such as galactose and to harmful chemicals such as copper ions. Only the pseudohyphae tips protrude from the ECM, but these are still protected by the MDR exporters. The tips may function as the sensors of nutrients and other environmental stimuli important to the colony. The questions remain as to what the chemical nature of the ECM is and how the embedded cells access the nutrients that are essential for their growth. It was previously shown that the ECMs of various microorganisms function as sorptive sponges that sequester organic molecules close to the cells (Decho, 2000) and that they also bind and sequester drugs (Nett et al., 2010). Yeast ECMs vary by their content of different polymeric and monomeric carbohydrates, proteins, and phosphorus (Al-Fattani and Douglas, 2006) and are even preferentially grazed by ciliates (Joubert et al., 2006), suggesting that ECMs have nutritional value. Thus, we hypothesize that in the biofilm colony, the ECM itself may function both as a sequestration barrier and a nutrient pool essential for new cell progeny within the cavities.

In conclusion, the specific architecture of the biofilm colony enables multiple protection strategies (Video 2), yielding a high level of resistance in the wild. Importantly, some of the colony features that we have shown here (e.g., a specific growth pattern, the production of the ECM, and drug efflux pumps) are the traits that are also implicated in the formation of complex fungal biofilms (Blankenship and Mitchell, 2006). The structured yeast colony thus represents a well-defined and powerful in vivo model system that may help to uncover the underlying general principles of microbial biofilm formation.

Materials and methods

Yeast strains and media

The wild yeast strain BR-F was supplied from a collection of the Institute of Chemistry (Slovak Academy of Sciences). The temperature-sensitive mutant strain ts104 was obtained from a collection of Charles University in Prague. All other strains were derivatives of the BR-F strain and were prepared in this study (Table I). Colonies were grown on GMA (3% glycerol, 1% yeast extract, and 2% agar) at 28°C unless otherwise indicated.

Strain constructs

Strains with gene deletions, C-terminal GFP fusions, and artificial-promoter (P_{CUP1} and P_{GAL1}) constructs replacing the *HIS3* gene were prepared according to Gueldener et al. (2002) and Sheff and Thorn (2004) by transforming the cells with DNA cassettes generated by PCR that used the primers and plasmids listed in Tables S1 and S2. The *cdc3-1* allele from the ts104 strain was first cloned into the pFA6a-natNT2 vector using BamHI and AscI restriction enzymes. The DNA cassette was then

Downloaded from http://rupress.org/jcb/article-pdf/194/5/679/1569090/jcb_201103129.pdf by guest on 06 December 2025

amplified and used to replace the wild-type *CDC3* allele in the BR-F–*cdc3CDC3* strain. Yeast cells were transformed as described by Gietz and Woods (2002).

Fluorescence microscopy of cells and colony imaging

Cells in the cultivation medium were examined at RT under a microscope (DMR; Leica) equipped with a 100×/1.3 oil objective and a GFP filter or Nomarski contrast and then photographed with a charge-coupled device camera (ProgRes MFcool; Jenoptik; Figs. 2 [A and B] and S2). Colony images were captured in incident light with a Navitar objective and a complementary metal-oxide semiconductor camera (ProgRes CT3; Jenoptik; Fig. S1 A). Time-lapse experiments were performed using a camera (DS-5M; Nikon) with a Navitar 12× objective and light-emitting diode illumination (Video 1). NIS-Elements software (Laboratory Imaging) was used throughout.

2P-CM

2P-CM (Figs. 1 [A–D], 2 [C and D], 3 [A–D and F], and 4 [A–C]) was performed according to Váchová et al. (2009). In brief, colonies were embedded in low-gelling agarose directly on the plates at RT and cut vertically down the middle. They were placed on the coverslip (the cutting edge to the glass), and the colony side views were obtained by 2P-CM. When required, the cross sections were stained with the following fluorescent dyes: 2.5 µg/ml NR, 30 µg/ml ConA-AF, and 1 µg/ml calcofluor white. Alternatively, GFP fluorescence was monitored. Images were acquired at RT with a true confocal scanner microscope (SP2 AOBS MP; Leica) fitted with a mode-locked laser (Ti:Sapphire Chameleon Ultra; Coherent Inc.) for two-photon excitation and using 20×/0.70 and 63×/1.20 water immersion plan apochromat objectives. Excitation wavelengths of 920 nm were used for ConA-AF, NR, and GFP, and wavelengths of 790 nm were used for calcofluor white. Emission bandwidths were set to 470–540 nm for ConA, 580–750 nm for NR, 480–595 nm for GFP, and 400–550 nm for calcofluor white. An overview of the morphology of colonies and individual cells was obtained simultaneously with green fluorescence as autofluorescence in the 600–740-nm wavelength range. Images of colonies older than 2 d were composed of two or three stitched fields of view. Details in Fig. 1 (B2 and C1) and Fig. 2 (D4) were obtained by composing two images from neighboring fields of view.

EM

Small blocks (~1 mm^3) of colonies embedded in a 2% agarose gel were fixed by glutaraldehyde/potassium permanganate according to Wright (2000) and embedded in PolyBed 812 (Polysciences, Inc.). Using a transmission electron microscope (1011; JEOL Ltd.) at 80 kV, 70-nm ultrathin sections (prepared on a Reichert-Jung ultramicrotome) stained by uranyl acetate and lead citrate were examined. Images (Figs. 1 E and S1 B) were acquired by a digital camera (MegaView III) and AnalySIS software (Olympus).

Online supplemental material

Fig. S1 shows the differences between parental BR-F and knockout BR-F–*flo11* strains. Fig. S2 shows the early production of Pdr5p-GFP. Tables S1 and S2 list primers and plasmids used in this study, respectively. Video 1 shows BR-F colony growth. Video 2 shows flash animations of biofilm colony development and defense strategies. Online supplemental material is available at http://www.jcb.org/cgi/content/full/jcb.201103129/DC1.

We thank Dr. R. Pelc for helpful comments on the manuscript and H. Žd'árská for technical assistance.

The study was supported by the Grant Agency of the Czech Republic (grant 204/08/0718 to Z. Palková and L. Váchová) and the Ministry of Education (grant LC531 to Z. Palková and L. Váchová; grant LC06063 to Z. Palková and L. Kubínová; grant MSM0021620858 to Z. Palková and V. Št'ovíček; grant AV0Z50200510 to L. Váchová and O. Hlaváček; and grant AV0Z50110509 to L. Kubínová). Z. Palková is a Howard Hughes Medical Institute International Research Scholar.

Submitted: 24 March 2011
Accepted: 1 August 2011

References

Al-Fattani, M.A., and L.J. Douglas. 2006. Biofilm matrix of *Candida albicans* and *Candida tropicalis*: chemical composition and role in drug resistance. *J. Med. Microbiol.* 55:999–1008. doi:10.1099/jmm.0.46569-0

Baillie, G.S., and L.J. Douglas. 2000. Matrix polymers of *Candida* biofilms and their possible role in biofilm resistance to antifungal agents. *J. Antimicrob. Chemother.* 46:397–403. doi:10.1093/jac/46.3.397

Balzi, E., W. Chen, S. Ulaszewski, E. Capieaux, and A. Goffeau. 1987. The multidrug resistance gene *PDR1* from *Saccharomyces cerevisiae*. *J. Biol. Chem.* 262:16871–16879.

Balzi, E., M. Wang, S. Leterme, L. Van Dyck, and A. Goffeau. 1994. *PDR5*, a novel yeast multidrug resistance conferring transporter controlled by the transcription regulator *PDR1*. *J. Biol. Chem.* 269:2206–2214.

Bayly, J.C., L.M. Douglas, I.S. Pretorius, F.F. Bauer, and A.M. Dranginis. 2005. Characteristics of Flo11-dependent flocculation in *Saccharomyces cerevisiae*. *FEM. Yeast Res.* 5:1151–1156. doi:10.1016/j.femsyr.2005.05.004

Beauvais, A., C. Loussert, M.C. Prevost, K. Verstrepen, and J.P. Latgé. 2009. Characterization of a biofilm-like extracellular matrix in *FLO1*-expressing *Saccharomyces cerevisiae* cells. *FEM. Yeast Res.* 9:411–419. doi:10.1111/j.1567-1364.2009.00482.x

Blankenship, J.R., and A.P. Mitchell. 2006. How to build a biofilm: a fungal perspective. *Curr. Opin. Microbiol.* 9:588–594. doi:10.1016/j.mib.2006.10.003

Decho, A.W. 2000. Microbial biofilms in intertidal systems: an overview. *Cont. Shelf Res.* 20:1257–1273. doi:10.1016/S0278-4343(00)00022-4

Donlan, R.M., and J.W. Costerton. 2002. Biofilms: survival mechanisms of clinically relevant microorganisms. *Clin. Microbiol. Rev.* 15:167–193. doi:10.1128/CMR.15.2.167-193.2002

Douglas, L.J. 2003. *Candida* biofilms and their role in infection. *Trends Microbiol.* 11:30–36. doi:10.1016/S0966-842X(02)00002-1

Douglas, L.M., L. Li, Y. Yang, and A.M. Dranginis. 2007. Expression and characterization of the flocculin Flo11/Muc1, a *Saccharomyces cerevisiae* mannoprotein with homotypic properties of adhesion. *Eukaryot. Cell.* 6:2214–2221. doi:10.1128/EC.00284-06

Dranginis, A.M., J.M. Rauceo, J.E. Coronado, and P.N. Lipke. 2007. A biochemical guide to yeast adhesins: glycoproteins for social and antisocial occasions. *Microbiol. Mol. Biol. Rev.* 71:282–294. doi:10.1128/MMBR.00037-06

Fardeau, V., G. Lelandais, A. Oldfield, H. Salin, S. Lemoine, M. Garcia, V. Tanty, S. Le Crom, C. Jacq, and F. Devaux. 2007. The central role of *PDR1* in the foundation of yeast drug resistance. *J. Biol. Chem.* 282:5063–5074. doi:10.1074/jbc.M610197200

Flemming, H.C., and J. Wingender. 2010. The biofilm matrix. *Nat. Rev. Microbiol.* 8:623–633.

Gietz, R.D., and R.A. Woods. 2002. Transformation of yeast by lithium acetate/single-stranded carrier DNA/polyethylene glycol method. *Methods Enzymol.* 350:87–96. doi:10.1016/S0076-6879(02)50957-5

Gimeno, C.J., P.O. Ljungdahl, C.A. Styles, and G.R. Fink. 1992. Unipolar cell divisions in the yeast *S. cerevisiae* lead to filamentous growth: regulation by starvation and RAS. *Cell.* 68:1077–1090. doi:10.1016/0092-8674(92)90079-R

Greenspan, P., and S.D. Fowler. 1985. Spectrofluorometric studies of the lipid probe, nile red. *J. Lipid Res.* 26:781–789.

Gueldener, U., J. Heinisch, G.J. Koehler, D. Voss, and J.H. Hegemann. 2002. A second set of loxP marker cassettes for Cre-mediated multiple gene knockouts in budding yeast. *Nucleic Acids Res.* 30:e23. doi:10.1093/nar/30.6.e23

Guo, B., C.A. Styles, Q. Feng, and G.R. Fink. 2000. A *Saccharomyces* gene family involved in invasive growth, cell-cell adhesion, and mating. *Proc. Natl. Acad. Sci. USA.* 97:12158–12163. doi:10.1073/pnas.220420397

Hartwell, L.H. 1971. Genetic control of the cell division cycle in yeast. IV. Genes controlling bud emergence and cytokinesis. *Exp. Cell Res.* 69:265–276. doi:10.1016/0014-4827(71)90223-0

Ishigami, M., Y. Nakagawa, M. Hayakawa, and Y. Iimura. 2004. *FLO11* is essential for flor formation caused by the C-terminal deletion of *NRG1* in *Saccharomyces cerevisiae*. *FEMS Microbiol. Lett.* 237:425–430.

Joubert, L.M., G.M. Wolfaardt, and A. Botha. 2006. Microbial exopolymers link predator and prey in a model yeast biofilm system. *Microb. Ecol.* 52:187–197. doi:10.1007/s00248-006-9063-7

Jungwirth, H., and K. Kuchler. 2006. Yeast ABC transporters–a tale of sex, stress, drugs and aging. *FEBS Lett.* 580:1131–1138. doi:10.1016/j.febslet.2005.12.050

Klis, F.M., G.J. Sosinska, P.W. de Groot, and S. Brul. 2009. Covalently linked cell wall proteins of *Candida albicans* and their role in fitness and virulence. *FEM. Yeast Res.* 9:1013–1028. doi:10.1111/j.1567-1364.2009.00541.x

Koning, A.J., C.J. Roberts, and R.L. Wright. 1996. Different subcellular localization of *Saccharomyces cerevisiae* HMG-CoA reductase isozymes at elevated levels corresponds to distinct endoplasmic reticulum membrane proliferations. *Mol. Biol. Cell.* 7:769–789.

Kuthan, M., F. Devaux, B. Janderová, I. Slaninová, C. Jacq, and Z. Palková. 2003. Domestication of wild *Saccharomyces cerevisiae* is accompanied by changes in gene expression and colony morphology. *Mol. Microbiol.* 47:745–754. doi:10.1046/j.1365-2958.2003.03332.x

Downloaded from http://rupress.org/jcb/article-pdf/194/5/679/1569090/jcb_201103129.pdf by guest on 06 December 2025

Lambrechts, M.G., F.F. Bauer, J. Marmur, and I.S. Pretorius. 1996. Muc1, a mucin-like protein that is regulated by Mss10, is critical for pseudohyphal differentiation in yeast. *Proc. Natl. Acad. Sci. USA*. 93:8419–8424. doi:10.1073/pnas.93.16.8419

Mukherjee, P.K., J. Chandra, D.M. Kuhn, and M.A. Ghannoum. 2003. Mechanism of fluconazole resistance in *Candida albicans* biofilms: phase-specific role of efflux pumps and membrane sterols. *Infect. Immun.* 71:4333–4340. doi:10.1128/IAI.71.8.4333-4340.2003

Nett, J.E., H. Sanchez, M.T. Cain, and D.R. Andes. 2010. Genetic basis of *Candida biofilm* resistance due to drug-sequestering matrix glucan. *J. Infect. Dis.* 202:171–175. doi:10.1086/651200

Nobile, C.J., H.A. Schneider, J.E. Nett, D.C. Sheppard, S.G. Filler, D.R. Andes, and A.P. Mitchell. 2008. Complementary adhesin function in *C. albicans* biofilm formation. *Curr. Biol.* 18:1017–1024. doi:10.1016/j.cub.2008.06.034

Palková, Z. 2004. Multicellular microorganisms: laboratory versus nature. *EMBO Rep.* 5:470–476. doi:10.1038/sj.embor.7400145

Ramage, G., S. Bachmann, T.F. Patterson, B.L. Wickes, and J.L. López-Ribot. 2002. Investigation of multidrug efflux pumps in relation to fluconazole resistance in *Candida albicans* biofilms. *J. Antimicrob. Chemother.* 49:973–980. doi:10.1093/jac/dkf049

Ramsook, C.B., C. Tan, M.C. Garcia, R. Fung, G. Soybelman, R. Henry, A. Litewka, S. O'Meally, H.N. Otoo, R.A. Khalaf, et al. 2010. Yeast cell adhesion molecules have functional amyloid-forming sequences. *Eukaryot. Cell*. 9:393–404. doi:10.1128/EC.00068-09

Reynolds, T.B., and G.R. Fink. 2001. Bakers' yeast, a model for fungal biofilm formation. *Science*. 291:878–881. doi:10.1126/science.291.5505.878

Rogers, B., A. Decottignies, M. Kolaczkowski, E. Carvajal, E. Balzi, and A. Goffeau. 2001. The pleitropic drug ABC transporters from *Saccharomyces cerevisiae. J. Mol. Microbiol. Biotechnol.* 3:207–214.

Servos, J., E. Haase, and M. Brendel. 1993. Gene *SNQ2* of *Saccharomyces cerevisiae*, which confers resistance to 4-nitroquinoline-N-oxide and other chemicals, encodes a 169 kDa protein homologous to ATP-dependent permeases. *Mol. Gen. Genet.* 236:214–218. doi:10.1007/BF00277115

Sheff, M.A., and K.S. Thorn. 2004. Optimized cassettes for fluorescent protein tagging in *Saccharomyces cerevisiae. Yeast*. 21:661–670. doi:10.1002/yea.1130

Sipos, G., and K. Kuchler. 2006. Fungal ATP-binding cassette (ABC) transporters in drug resistance & detoxification. *Curr. Drug Targets*. 7:471–481. doi:10.2174/138945006776359403

Smukalla, S., M. Caldara, N. Pochet, A. Beauvais, S. Guadagnini, C. Yan, M.D. Vinces, A. Jansen, M.C. Prevost, J.P. Latgé, et al. 2008. *FLO1* is a variable green beard gene that drives biofilm-like cooperation in budding yeast. *Cell*. 135:726–737. doi:10.1016/j.cell.2008.09.037

Šťovíček, V., L. Váchová, M. Kuthan, and Z. Palková. 2010. General factors important for the formation of structured biofilm-like yeast colonies. *Fungal Genet. Biol.* 47:1012–1022. doi:10.1016/j.fgb.2010.08.005

Tokunaga, M., M. Kusamichi, and H. Koike. 1986. Ultrastructure of outermost layer of cell wall in *Candida albicans* observed by rapid-freezing technique. *J. Electron Microsc. (Tokyo)*. 35:237–246.

Uppuluri, P., A.K. Chaturvedi, and J.L. Lopez-Ribot. 2009. Design of a simple model of *Candida albicans* biofilms formed under conditions of flow: development, architecture, and drug resistance. *Mycopathologia*. 168:101–109. doi:10.1007/s11046-009-9205-9

Váchová, L., O. Chernyavskiy, D. Strachotová, P. Bianchini, Z. Burdíková, I. Fercíková, L. Kubínová, and Z. Palková. 2009. Architecture of developing multicellular yeast colony: spatio-temporal expression of Ato1p ammonium exporter. *Environ. Microbiol.* 11:1866–1877. doi:10.1111/j.1462-2920.2009.01911.x

Verstrepen, K.J., T.B. Reynolds, and G.R. Fink. 2004. Origins of variation in the fungal cell surface. *Nat. Rev. Microbiol.* 2:533–540. doi:10.1038/nrmicro927

Vopálenská, I., V. Šťovíček, B. Janderová, L. Váchová, and Z. Palková. 2010. Role of distinct dimorphic transitions in territory colonizing and formation of yeast colony architecture. *Environ. Microbiol.* 12:264–277. doi:10.1111/j.1462-2920.2009.02067.x

Wolfger, H., Y. Mahé, A. Parle-McDermott, A. Delahodde, and K. Kuchler. 1997. The yeast ATP binding cassette (ABC) protein genes *PDR10* and *PDR15* are novel targets for the Pdr1 and Pdr3 transcriptional regulators. *FEBS Lett.* 418:269–274. doi:10.1016/S0014-5793(97)01382-3

Wright, R. 2000. Transmission electron microscopy of yeast. *Microsc. Res. Tech.* 51:496–510. doi:10.1002/1097-0029(20001215)51:6<496::AID-JEMT2>3.0.CO;2-9

Zara, G., S. Zara, C. Pinna, S. Marceddu, and M. Budroni. 2009. *FLO11* gene length and transcriptional level affect biofilm-forming ability of wild flor strains of *Saccharomyces cerevisiae. Microbiology*. 155:3838–3846. doi:10.1099/mic.0.028738-0

Downloaded from http://rupress.org/jcb/article-pdf/194/5/679/1569090/jcb_201103129.pdf by guest on 06 December 2025